

Ion source backplate loading due to backstreaming electrons and the arc discharge in the JET EP2 neutral beam injectors



I. Turner*, R. McAdams, W. Arter, A. Ash, M. Barnard, D. Ćirić, I. Day, D. Keeling, D. King, C. Lane, M. Nicassio, T. Robinson, A. Shepherd, J. Zacks

United Kingdom Atomic Energy Authority, Culham Centre for Fusion Energy, Culham Science Centre, Abingdon, Oxon, OX14 3DB, UK

ARTICLE INFO

Keywords:

Neutral beam injection
Ion source
Backplate
Backstreaming electrons
JET

ABSTRACT

The neutral beam power into JET can be increased by increasing the neutraliser gas flow (and gas pressure), hence ensuring a higher neutralisation efficiency. This has the potential to increase the loading on the ion source backplate due to backstreaming electrons. Measurements of the total backplate power loading due to backstreaming electrons and also the arc discharge are presented for the JET EP2 neutral beam injectors as the neutraliser gas flow rate is varied. The measurements are carried out for normal gas delivery operation and for the gas delivery method (grid gas delivery) that is required for the production of tritium beams at JET. Modelling of the backstreaming electron power load and the power distribution is also carried out and the former is compared to the experimental measurements. The backplate loading is more sensitive to the gas flow rate in the case of grid gas delivery. The measurements and calculations can be used to understand the thermo-mechanical performance of the system to balance the benefit of increased neutral beam power against potential increased fatigue and reduced lifetime of the backplate.

1. Introduction

The Joint European Torus (JET) has two neutral beam heating boxes. Each box consists of eight Positive Ion Neutral beam Injectors (PINIs). The latest design of the PINIs are designated EP2 [1]. These consist of an ion source and accelerator rated at up to 125 kV, 65A operating in deuterium. The neutral beam power is 2.1 MW giving a total power of up to 34 MW in deuterium. The PINIs have been normally operated with an ion source gas flow of 10–14 mbar l/s and a neutraliser gas flow rate of 20 mbar l/s. Recent experiments have shown that it is possible to increase the injected neutral beam power by increasing the neutraliser gas flow rate. This is illustrated in Fig. 1 with deuterium plasma and beams, for two injectors (PINIs 4.1 and 4.4) operated at neutraliser flow rates of 20 and 30 mbar l/s. The data shows the (a) the extracted ion beam power, (b) the neutron rate from the plasma and (c) the ratio of the neutron rate for the two pulses with the different neutraliser gas flow rates. Pulse #92,250 used a neutraliser gas flow rate of 20 mbar l/s and pulse #92,247 used a neutraliser flow rate of 30 mbar l/s. For the target plasmas used, fusion reactions and thus neutron production, are primarily beam-target with a negligible thermal component. The increase in observed neutron production is therefore almost directly proportional to an increase in NBI particle

flux. Although there is a small increase in extracted ion beam power of < 2% between the two pulses, increasing the neutraliser gas flow rate increases the neutron rate by ~10% which represents a potential increase of a few MW in total JET neutral beam power. This increase in power has been confirmed by neutralisation measurements and a complete report on the increase in power will be the subject of a future paper [2].

Whilst an increase in injected neutral beam power is welcome for experimental campaigns and is accompanied by a reduction in power on the residual ion dumps, it may have detrimental consequences also. Higher gas flow to the neutraliser may well lead to higher power from backstreaming electrons formed by ionisation of the gas in the accelerator. These backstreaming electrons, which can have energies greater than the beam energy, predominantly strike the ion source backplate leading to possible increased fatigue and reduced lifetime and possibly even a water or vacuum breach. Measurement of the total backplate power loading due to the backstreaming electrons as well as the arc discharge is the subject of this report.

In Section 2 the method of measurement of the backplate power loading is described together with details of how the contribution from heating by the arc discharge can be subtracted out to give the contribution from the backstreaming electrons. Also, in this section,

* Corresponding author.

E-mail address: ingrid.turner@ukaea.uk (I. Turner).

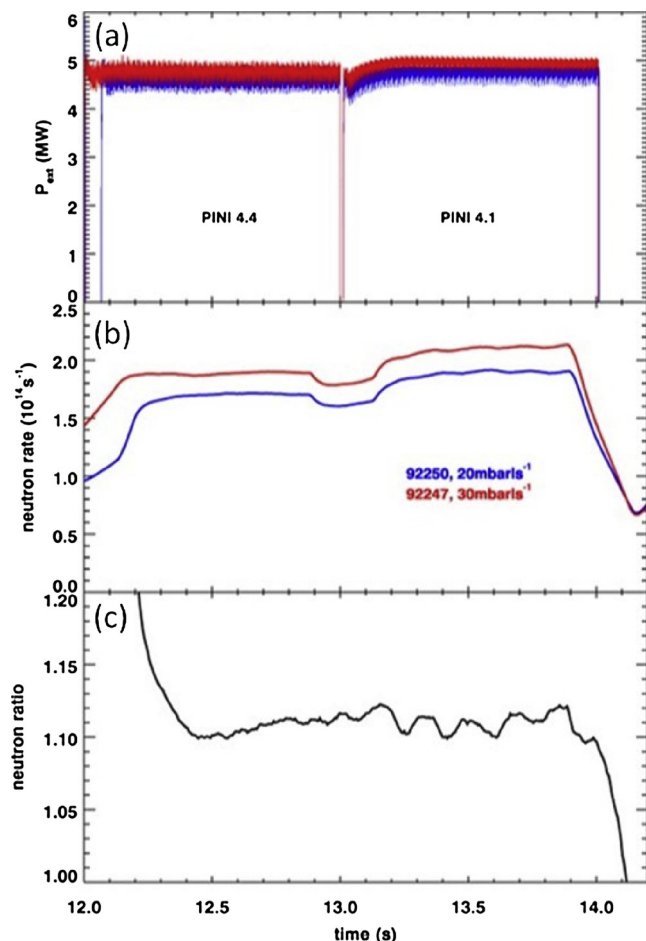


Fig. 1. (a) The extracted ion beam power, (b) neutron rates and (c) the ratio of neutron rates for two PINIs (4.1 and 4.4) at the different neutraliser gas flow rates for two JET pulses with different neutraliser gas flow rates: #92250 (20 mbar l/s) and #92247 (30 mbar l/s).

modelling is presented not only of the power of the backstreaming electrons but also of their spatial power distribution on the backplate. Such a calculation is useful in comparing with the backplate power measurements and the distribution can also be used as part of a thermo-mechanical analysis of the backplate under operational conditions to understand possible failure mechanisms and the operational lifetime. In Section 3, the measurements made are reported including comparisons with the modelling. The measurements are carried out for normal operation where the ion source and neutraliser have separate gas feeds and also for operation in grid gas mode where there is only one gas feed serving both the ion source and neutraliser [3,4]. This latter method of operation is required at JET for the production of tritium beams for future TT and DT campaigns. Finally some conclusions are drawn in Section 4.

2. Ion source backplate power loading

2.1. Measurement method for the backplate power loading

Fig. 2 shows the arc discharge (arc current and arc voltage) together with the beam extraction voltage and current for a 3.5 s pulse at 100 kV.

The power to the ion source backplate is measured calorimetrically. The cooling water flow rate to the backplate is measured separately from the remainder of the source body and also the plasma facing grid with the 262 extraction apertures (designated G1). The flow rate of the cooling water is measured together with the water temperature rise during a beam pulse (by a thermocouple). The energy measured, Q , is

given by

$$Q = \rho FC \int_0^{\infty} \Delta T(t) dt \quad (1)$$

where ρ is the density of water, F is the volumetric flow rate of the cooling water through the backplate, C is the specific heat capacity of water, and $\Delta T(t)$ is the measured temperature rise on the thermocouple. Fig. 3 shows a typical thermocouple response during a 3.5 s beam pulse.

The temperature rise is due to backstreaming electrons and heating of the backplate by the arc discharge. The water temperature starts to rise before the beam is switched on. This is because the arc discharge is established before beam turn-on and continues through the pulse as seen in Fig. 2. The effect of the filaments being switched on before the arc is a very small effect.

To determine the power of the backstreaming electrons the energy deposited on the backplate is measured for different beam pulse durations, τ , within a fixed duration of 5 s for the arc discharge and beam extraction. Fig. 2 shows that there is a step in arc voltage and in arc current when the beam is switched on. This is to assist the beam switch on process without HV breakdown. In order to separate the arc and backstreaming electron contributions, it is first necessary to determine the energy delivered to the backplate directly by the arc, accounting for the arc voltage step. This was done by running two otherwise identical 5 s duration arc-only pulses (i.e. with no extracted beam) with current and voltage set to the levels used before the arc voltage step and after the arc-voltage step respectively. The energy delivered to the backplate by the arc in each case was measured using water calorimetry as described above. The energy delivered to the backplate by the arc, E_{arc} , during a 5-second pulse, with beam duration τ is then straightforwardly determined by:

$$E_{arc} = \frac{\tau}{5} E_s + \frac{(5 - \tau)}{5} E_{ns} \quad (2)$$

where E_s is the energy measured during a pulse at arc discharge values when the step is present and E_{ns} is the measured energy during a pulse with the arc discharge values with no arc voltage step present.

This arc contribution can then be subtracted from the arc plus beam pulse energy to give the contribution from the backstreaming electrons. An example of such a measurement at 100 keV beam energy is shown in Fig. 4. The power of the backstreaming electrons is then found by applying a linear fit to the energy loading vs time data and taking the gradient - in the case shown this is ~ 81 kW. Measurements were made at beam energies up to 115 keV and for beam pulse durations of up to 3.5 s at a range of neutraliser gas flow rates and also grid gas flow rates. At the higher voltages, as well as being close to the limits of the NBTB power supply, the beam pulse duration was restricted to a maximum of 2 s due to the heating of beamline components. Increasing the beam energy would have meant reducing the maximum beam pulse duration further thus increasing the uncertainty in the power measurements.

The same technique can also be applied in future to other suitably instrumented components such as the source body i.e. the side walls and the extraction grid to obtain the power loading.

2.2. Calculation of the backplate loading distribution

In addition to measuring the total power due to backstreaming electrons it is also important to try to understand the distribution of that power. Such knowledge can be used in a mechanical and thermal engineering analysis of the backplate behavior to predict possible failure modes and lifetime. There are two sources for the backstreaming electrons: electrons produced by ionisation of the gas in the accelerator and production by secondary emission due to backstreaming ions created downstream of the accelerator striking surfaces in the accelerator.

2.2.1. Electrons from gas ionisation

In the case of electrons produced by ionisation of the gas in the

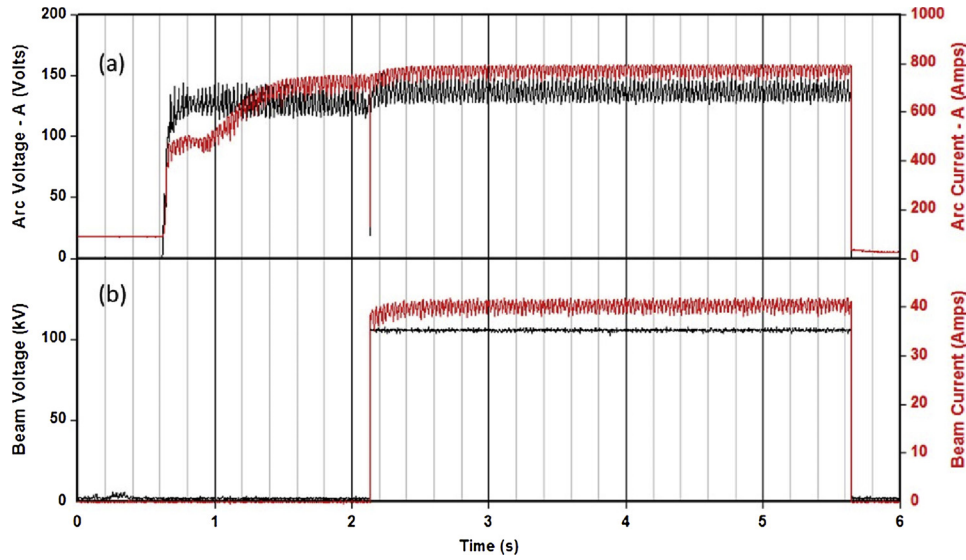


Fig. 2. The (a) arc discharge and (b) beam extraction waveforms for a 100 kV, 40A pulse.

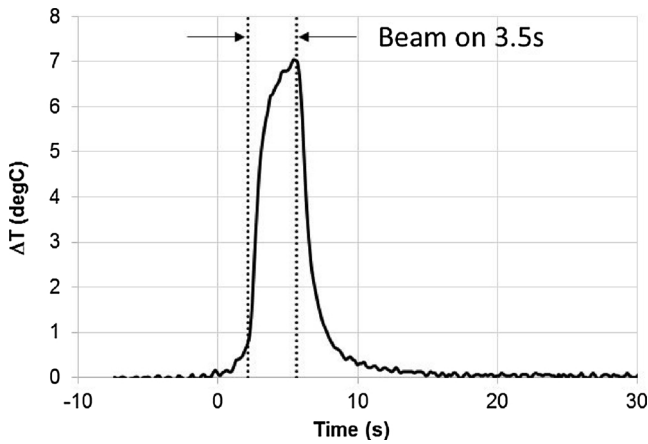


Fig. 3. Backplate cooling water thermocouple response during a 3.5 s beam pulse.

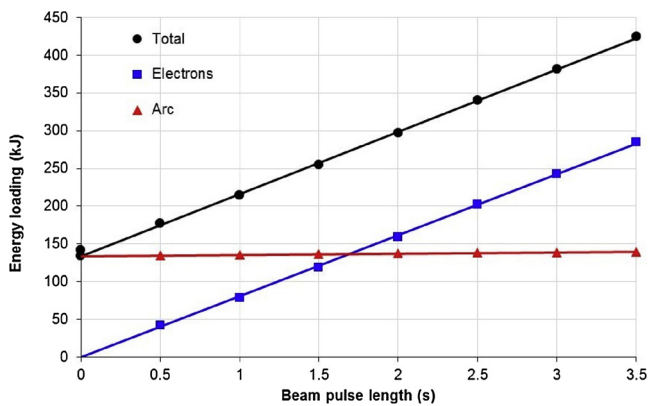


Fig. 4. Measured backplate energies for a 100 kV, 40A beam.

accelerator, the relative number of electrons, $dN(z)$ produced by ionisation of the background gas by the beam in the accelerator at a position z within a short distance dz around z is given by:

$$dN(z) \propto n_g(z)\sigma(E)dz \quad (3)$$

where z is along the beam axis, $n_g(z)$ is the gas density at z and $\sigma(E)$ is the ionisation cross-section at the energy of the beam E at the position

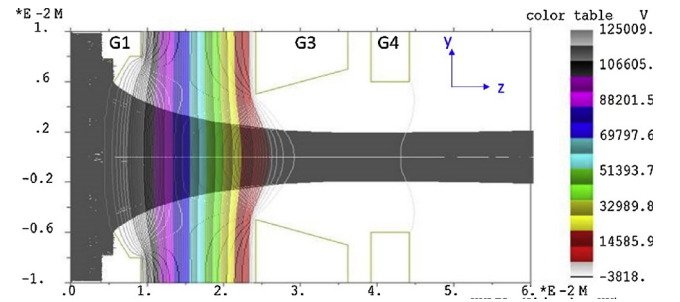


Fig. 5. AXCEL plot of the EP2 triode accelerator for a 125 kV, 60A deuterium beam.

z . Fig. 5 shows the triode accelerator design for one of the 262 extraction apertures of the EP2 injectors using the AXCEL code [5] for a 125 kV, 60A deuterium beam. The first grid at the left of Fig. 5 is the extraction or plasma grid (G1) and it has a potential of 125 kV. The second grid is the electron suppressor grid (designated G3) has a potential of -4 kV and the third grid is the earth grid (designated G4). This potential of -4 kV produces a barrier to prevent electrons produced downstream of G3 from reaching the backplate. At lower G3 voltages there is a sharp onset of backstreaming electrons. The potential map from the code allows the beam energy and hence the ionisation cross-section at any position z to be found.

Jones et al. [3] have given an empirical expression for the gas pressure at the earth grid, P_{grid} , for PINI types in use at the time

$$P_{grid}(Pa) = A_2^1 [0.348(F_s - F_{acc})^{0.96} + 0.126F_n^{0.94} - 0.0336(F_s - F_{acc})^{0.6}F_n^{0.94}] \quad (4)$$

where A is the isotopic mass, F_s is the gas flow rate supplied to the ion source, F_{acc} is the gas flow rate equivalent of the beam ions and F_n is the gas flow rate to the neutraliser. The measurements used to determine this empirical relationship would have had high pumping speeds outside of the neutralizer region, such that the pressures in the accelerator region would be determined by the accelerator and neutralizer conductance, as well as the flow rates to the source and neutralizer. The gas flow rates in this equation are in units of $Pa\ m^3\ s^{-1}$. Note that this equation is only valid for $F_s > F_{acc}$. Although it is expected that there will be some dependency of gas pressure on axial distance through the accelerator, for this calculation it is assumed that the pressure is uniform throughout the accelerator. Using this assumption, the relative number of electrons produced by ionization can be calculated at any

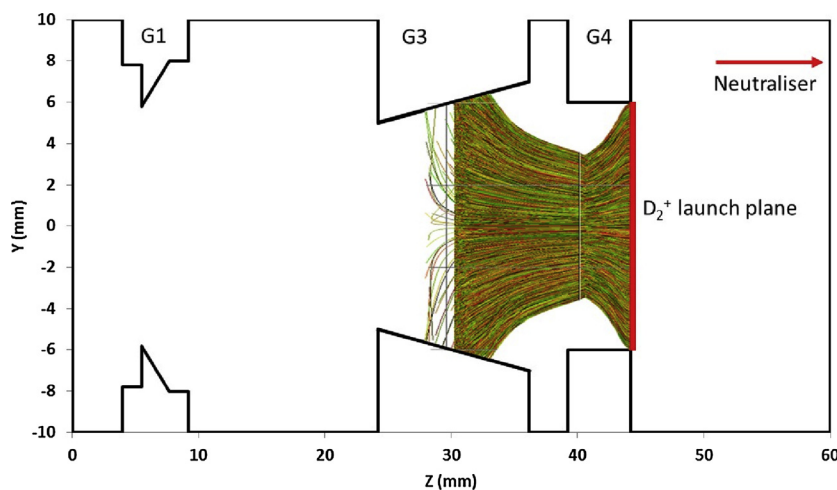


Fig. 6. Trajectories of D_2^+ ions from the neutraliser region.

distance from the source in the accelerator. This process needs to be repeated for all three components of the beam namely D^+ , D_2^+ , and D_3^+ . For a 125 keV, 60A beam the flux fractions were taken as $D^+ : D_2^+ : D_3^+ = 0.73 : 0.22 : 0.05$. This then gives the total electron current produced at each plane. This is repeated for many planes at 1 mm intervals and the electrons produced are tracked as described later.

2.2.2. Electrons from secondary emission

When the beam enters the neutraliser region beyond the accelerator it will ionise a portion of the background gas. Inspection of the cross-sections together with the flux fractions shows that D_2^+ is most likely to be produced in ionising collisions with the background gas. The D_2^+ ions can be accelerated between the earth grid and Grid 3. If they strike accelerator grids secondary electrons can be produced and potentially contribute to the backstreaming flux. Secondary electrons could also be produced by direct beam strike on grids but this potential contribution has been neglected, as this can be justified by Fig. 5 which shows that, when well focused, the beam is not close to the grids. In Fig. 6 the trajectories of D_2^+ ions produced in the neutraliser region have been tracked in the electrostatic potential map of the accelerator. The ions have been assumed to have been created with very low energy. It is clear from the trajectories that the ions strike grid 3 at close to normal incidence in an area of small axial extent but spread azimuthally around the grid.

Secondary electrons can then be launched from the region where the ions strike G3 and tracked through the accelerator. Fubiani [6] suggests that secondary electrons are emitted from the grid surface with random velocity vectors and with energies of ~ 10 eV. Fig. 7 shows trajectories of secondary electrons launched in random directions with an energy of 10 eV from the positions on Grid 3 where D_2^+ ions strike. Most of the electrons are accelerated towards grid 4 and the remainder towards grid 1. From the trajectory data produced by the tracking code it was possible to determine the fraction, f , of backstreaming electrons out of the total number launched. In total 9720 electrons were launched and 582 of these were found to backstream to the source giving a value of $f = 0.06$ i.e. $\sim 6\%$.

The Grid 3 current can be considered to be made up from the ions coming from the neutraliser and the secondary electrons produced by those ions which are accelerated towards the earth grid. This current, I_{G3} , can then be written as:

$$I_{G3} = [1 + \gamma] I_{D_2^+} \quad (5)$$

where γ is the secondary electron emission coefficient at the Grid 3 voltage and $I_{D_2^+}$ is the D_2^+ ion current. The grid 3 current was measured from a high power JET pulse with G1 voltage of 124 kV which gave a G3 current of 7.5A at a Grid 3 voltage of 3.8 kV. For 3.8 keV D_2^+

impact, γ was found to be 0.134, by interpolation of data in [7] giving a D_2^+ current of ~ 6.6 A.

Finally the backstreaming secondary electron current, I_{se} , can be calculated using Eq. 6

$$I_{se} = f \gamma I_{D_2^+} \quad (6)$$

Using the above values, $I_{se} = 0.053$ A. Given that backstreaming electrons from Grid 3 are accelerated up to ~ 129 keV when the Grid 1 voltage = 125 kV, this current gives a total power at the extraction aperture of 6.9 kW, or ~ 26 W per extraction aperture. As will be shown below, this is small compared to the total power of backstreaming electrons formed by ionisation of the background gas i.e. ~ 300 kW. So secondary electron emission has been neglected in the power distribution calculation for the backstreaming electrons.

2.2.3. Ion source backplate power loading

From the planes through the accelerator in which the amount of ionisation is calculated, 1,266,442 backstreaming electrons were tracked back to the grid 1 aperture opening. The calculation was carried out for a PINI gas flow of 14 mbar l/s and a neutraliser gas flow rate of 20 mbar l/s with a beam energy of 125 kV and 60A of beam current. Fig. 8 shows the velocity distribution for these particles over a single extraction aperture. The highest energy particles are concentrated towards the centre of the aperture with only $\sim 10\%$ having energies over 100 keV. The total backstreaming electron power reaching the extraction aperture for this case is 301 kW i.e. 1.15 kW per aperture.

Having reached the extraction aperture, the backstreaming electrons must traverse the ion source. There are 262 extraction apertures in the plasma facing grid to deal with. The electrons are also subject to the magnetic fields of the confinement magnets on the ion source walls and backplate. In order to track this number of electrons the SMARRDA/NUCODE [8,9] approach has been used. The PINI ion source permanent magnets are in chequerboard configuration to enhance production of molecular ions [1]. The magnetic field from the array of permanent magnets has been calculated using the PerMag code [10]. Fig. 9 shows the magnetic field components of the ion source magnets at the backplate. The z-component is out of the plane of the image. The centres of the extraction apertures are marked by the + symbols. Due to the chequerboard configuration the magnetic fields in the source are short range and so will have negligible effect on the calculation of the backstreaming electron trajectories as far as the extraction apertures.

In Fig. 10 the power distribution on the backplate from SMARRDA/NUCODE is shown. The distribution is for only one half of the extraction grid, i.e. 131 apertures. The magnetic cusp pattern is clearly observed indicating that many of the electrons are corralled by the magnetic field

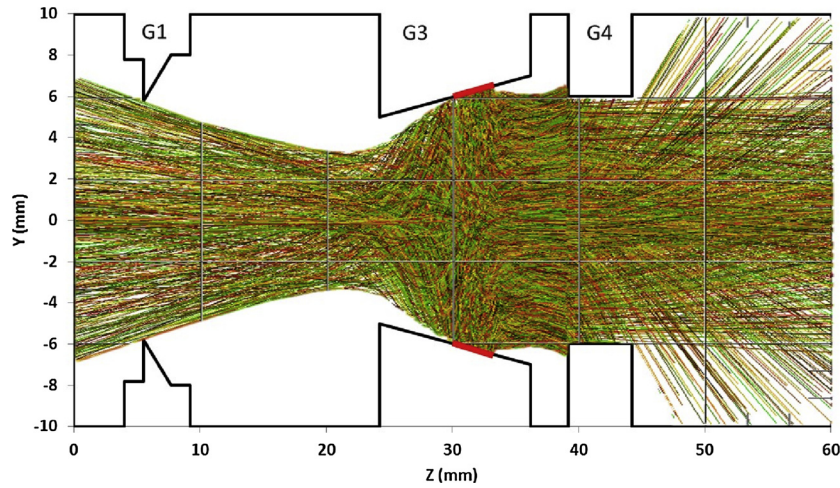


Fig. 7. Secondary electron trajectories for electrons launched at 10 eV with random velocity vectors w.r.t the G3 surface. Red markers indicate the launch area (For interpretation of the references to colour in this figure legend, the reader is referred to the web version of this article).

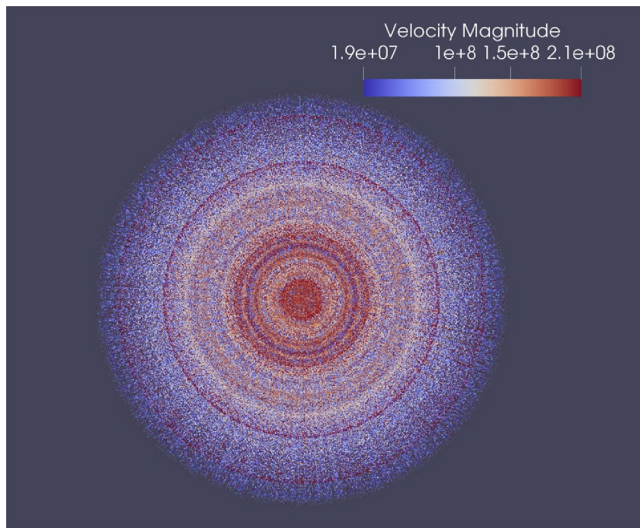


Fig. 8. The initial velocity distribution for the backstreaming electrons at Grid 1.

near the backplate to the cusps. The peak power density calculated is $\sim 14.9 \text{ MW m}^{-2}$ in a single mesh cell - this is likely to be unsustainable by current backplate cooling technology but is thought to be conservative, therefore improved meshing is required to improve the

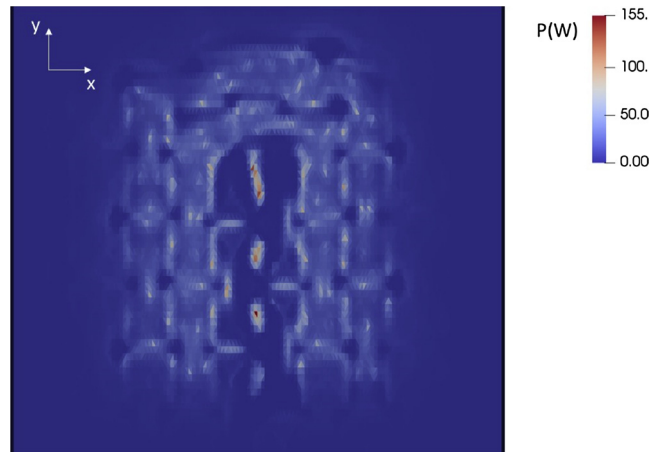


Fig. 10. The power distribution (in Watts) of the backstreaming electrons on the backplate for one half of the extraction apertures.

calculations for future use. This distribution can then be used along with the arc discharge power loading as part of a thermo-mechanical analysis of the backplate performance. The power on the backplate due to the backstreaming electrons is 230 kW. Thus in this calculation $\sim 76\%$ of the backstreaming electrons reach the backplate, the remainder striking the source side walls and the extraction grid.

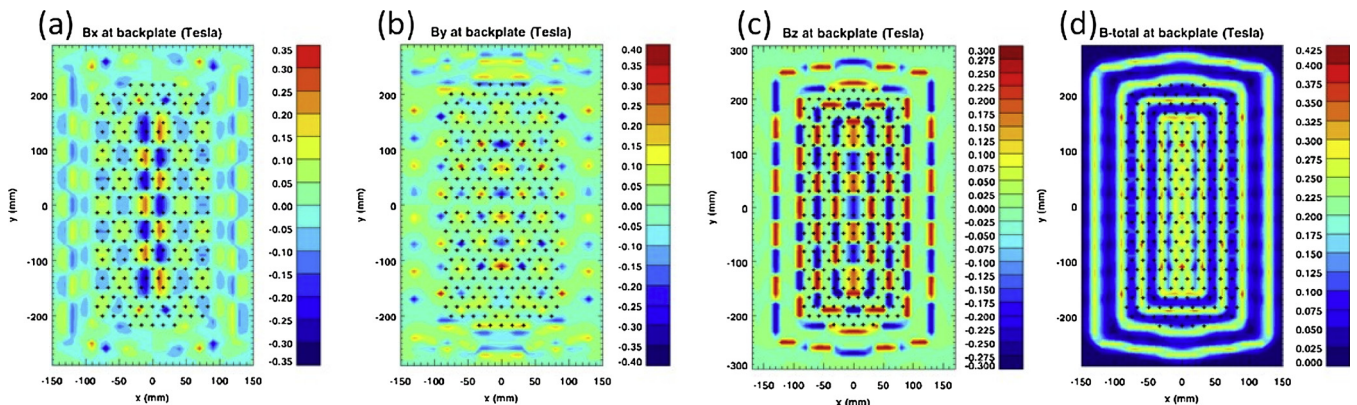


Fig. 9. The magnetic field components of the ion source magnets at the backplate; (a) Bx, (b) By, (c) Bz, (d) B total. The + symbols represent the positions of the extraction apertures.

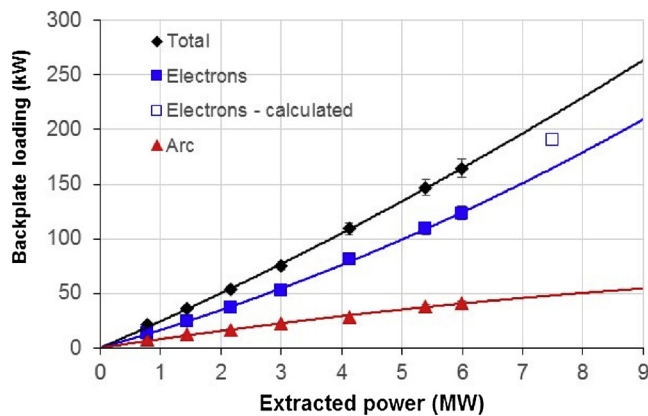


Fig. 11. Backplate power loadings for an ion source gas flow rate of 12 mbar l/s and a neutraliser gas flow rate of 20 mbar l/s.

3. Power loading measurements

3.1. Normal gas operation

Normal gas operation is the conventional method of delivering gas to the ion source and neutraliser where the gas feeds to the ion source and neutraliser are separate. For the PINIs the ion source gas is delivered into the back of the ion source and the neutraliser gas is delivered at a point about half way along the neutraliser. Typically the PINI gas flow rate is 10–14 mbar l/s and the neutraliser flow rate is usually 20 mbar l/s. As shown earlier there could be a desire to increase the neutraliser flow rate to increase the neutral beam power to JET. For a 60A beam current with flux fractions $D^+ : D_2^+ : D_3^+ = 0.73 : 0.22 : 0.05$, the beam represents a gas flow rate out of the ion source of ~ 10 mbar l/s of D_2 . This is replenished by the gas flow entering the ion source. The flow of gas to the ion source, neutraliser and the beam extraction determine the gas distribution in the accelerator.

In Fig. 11 the backplate power loading measured using the technique described in section 2.1 is shown as the extracted power is varied for a gas flow of 12 mbar l/s to the ion source and 20 mbar l/s to the neutraliser. The lines are empirical quadratic fits to the data. The highest extracted power in the dataset, for the reasons given earlier, is 6 MW. The fits can be used to extrapolate to full power i.e. 125 kV, 65A or 8.13 MW. The error bars on the points were determined from a combination of the error in the flow meter measurement ($\pm 2\%$) and the error in each point of the thermocouple trace ($\pm 0.05^\circ\text{C}$) in calculating the integral in Eq. 1 and the fit to the energy data. This gives a total error of 5%. At the highest extracted powers the loading due to the arc is $\sim 1/3$ of the loading due to the backstreaming electrons.

Also shown on the plot in Fig. 11 are the results of the SMARRDA/NUCODE calculation. This calculation was carried out at a gas flow rate of 14 mbar l/s for the ion source and 20 mbar l/s for the neutraliser at 125 kV, 60A giving a power of 230 kW to the backplate. The point on the graph for the calculation is this value scaled using Eq. 4 to an ion source gas flow rate of 12 mbar l/s. At the higher ion source gas flow rate of the calculation the gas pressure in the accelerator would be higher than for the lower gas flow rate. Given that a 60A beam represents an equivalent gas flow rate of 10 mbar l/s the maximum the pressure could increase by is $(14-10)/(12-10)$ or a factor of 2 although this does not account for the neutraliser gas. The scaling gives a pressure decrease at the earth grid of 17% when reducing the ion source gas flow rate from 14 to 12 mbar l/s. The calculation fits relatively well with the data trend.

The combined measured loadings for the source body and G1 together are shown in Fig. 12. In this case the calculated loading is taken as that which does not strike the backplate. The calculated value lies below the data trend in this case although the measured G1 power may

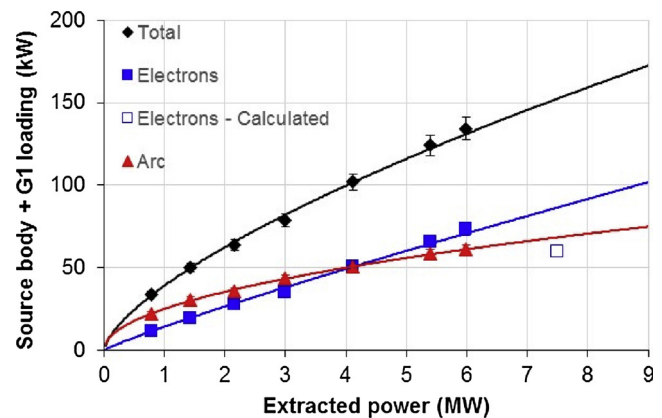


Fig. 12. Source body and G1 combined power loadings for an ion source gas flow rate of 12 mbar l/s and a neutraliser gas flow rate of 20 mbar l/s.

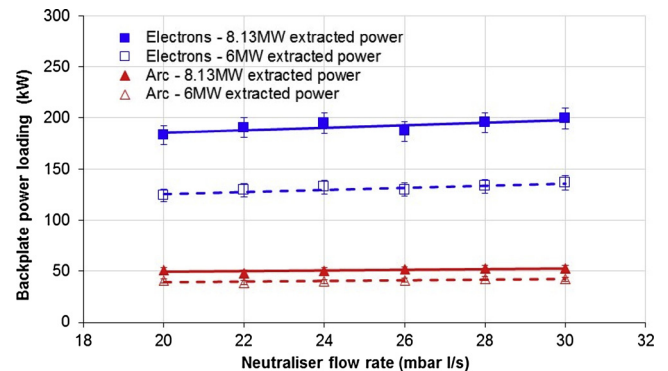


Fig. 13. Backplate loading due to backstreaming electrons and the arc as the neutraliser gas flow rate is varied for an ion source gas flow rate of 12 mbar l/s.

have a contribution from the beam.

The effect of changing the neutraliser gas flow rate for a fixed ion source gas flow rate of 12 mbar l/s on the backplate loading due to the backstreaming electrons and the arc is shown in Fig. 13. Two examples are shown. The data at the highest measured extracted power of 6 MW (115 kV, 52A) is shown along that for full extracted power of 8.13 MW (125 kV, 65A) obtained from the extrapolation of the measurements as in Fig. 11. The arc discharge power is constant as the neutraliser gas flow is varied over this range. Increasing the neutraliser gas flow from 20 to 30 mbar l/s increases the loading by 9% at full extracted power whilst the arc power loading remains constant. Use of Eq. 4 estimates a rise in the pressure at the earth grid of $\sim 28\%$ which is higher than that observed although details of the gas distribution may be important.

3.2. Grid gas operation

Operation of the PINIs in grid gas mode refers to the mode of operation where the gas to the ion source and neutraliser are supplied by a single gas feed at the earth grid [3,4]. Such operation is necessary at JET to produce tritium beams. This is because the ion source gas feed passes through towers in an insulating break, with other PINI services, with gas insulation in the towers to prevent breakdowns. These towers do not act as secondary containment in the event of a tritium leak. It proved a difficult challenge to engineer such a gas feed with secondary containment. The Neutral Beam Test Bed cannot be operated with tritium beams and so backplate load measurements in grid gas mode were carried out in deuterium.

Fig. 14 shows the backplate loadings for grid gas operation at a grid gas flow rate of 30 mbar l/s. The highest extracted power is for a beam voltage of 110 kV and beam current of 48A. In comparison with Fig. 11,

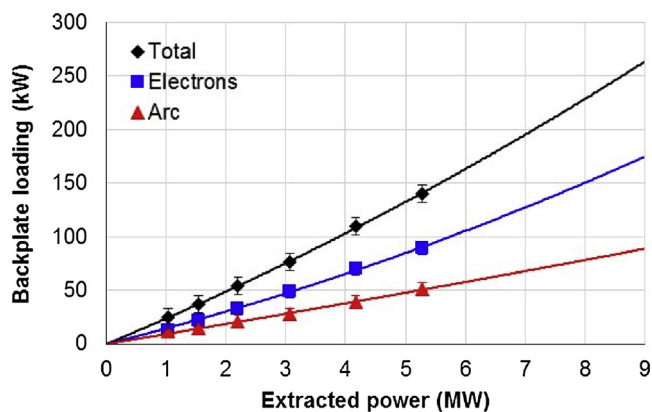


Fig. 14. Backplate power loadings for a grid gas flow rate of 30 mbar l/s.

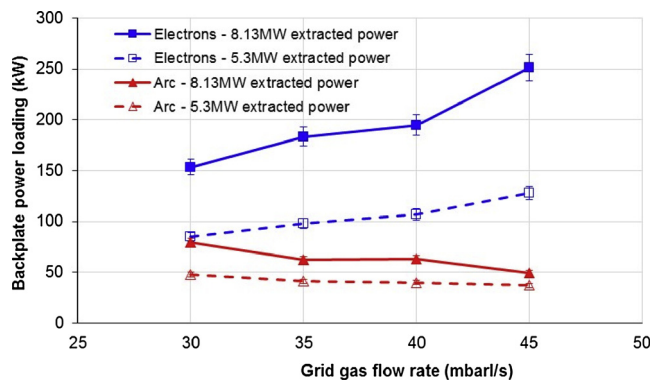


Fig. 15. Backplate loading due to backstreaming electrons and the arc as the grid gas flow rate is varied.

the trends are very similar although in this case the backplate loadings are a little lower for the particular flow rate illustrated.

The dependence of the loadings as the grid gas flow rate is changed is shown in Fig. 15. The data is shown for an extracted power of 5.3 MW and for an extrapolated power of 8.13 MW. The behaviour of the power loading is noticeably different from that for normal gas operation as shown in Fig. 12. At lower grid gas flow rates the power loading for the backstreaming electrons is lower compared to normal gas operation at the same total gas flow rate. At higher grid gas flow rates the loading is higher than the same total gas flow rate in normal operation. This must be due to the gas pressure distribution in the accelerator.

For the backstreaming electrons the power loading is increased by ~64% for 8.13 MW extracted power and 51% for 5.3 MW extracted power when the grid gas flow is increased from 30 to 45 mbar l/s. This change is considerably larger than for the normal gas operation case where the increase was more modest at ~9% over almost the same range of total gas flow rate to the PINI. In normal gas operation, at high currents (~60A) the ion beam represented a high proportion of the gas flow rate from the PINI. This effective outflow of gas is replenished primarily through the ion source gas feed. In grid gas operation the beam represents ~1/3-1/4 of the grid gas flow rate. There is no ion source gas feed and the source is replenished by a gas flow from the earth grid through the accelerator grid to the ion source [3,4]. Thus the pressure distribution would be different. Eq. 4 [3] was found to be applicable in both normal gas and grid gas operation. In the latter case the neutraliser gas flow rate is set to zero and F_s is the grid gas flow rate. Using values for grid gas flow rates of 30 and 35 mbar l/s the pressure at the earth grid increases by 71% in reasonable agreement with the measured increases in loading over that range. From Eq. 3 it would be expected that the power loading is in direct proportion with the gas pressure.

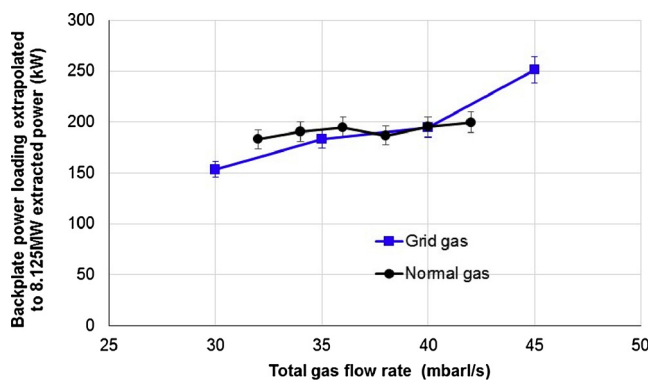


Fig. 16. Comparison of backplate loading due to backstreaming electrons for normal and grid gas operation. The loading is plotted against total gas flow rate to the ion source and neutralizer.

Fig. 16 shows a comparison of the backplate loading for normal gas and grid gas operation. The loading is plotted against the total gas flow to the ion source and neutraliser in each mode of operation. The ion source gas flow rate in normal operation is 12 mbar l/s. At the lower total gas flow rates the normal gas operation has a higher loading whereas the situation is reversed at higher total flow rates. Presumably this is due to changes in the pressure distribution in the accelerator. The operating point in tritium is not yet known. It is probably at grid gas flow rates of > 25 mbar l/s [4]. Determination of this operating point requires operation of the injectors in tritium on JET to measure arc efficiency, neutralisation, species and voltage holding.

The power loading due to the arc decreases as the grid gas flow rate increases. In the normal gas operation case the arc power required to produce a beam of fixed ion current remained constant. In the grid gas operation case, at lower grid gas flow rates a higher arc current is required to produce a given beam current than at higher arc grid gas flow rates. This is illustrated in Fig. 17 where the arc loading for 5.3 MW extracted power is shown together with its ratio to the actual arc discharge power. The contribution of the arc to the backplate loading is approximately a constant fraction of the arc power. This lower arc efficiency at lower grid gas flow rates is a feature of grid gas operation as demonstrated previously [4] and it has other effects such as changing the ion species fractions.

4. Conclusions

The measurements of the backplate power due to backstreaming electrons in normal gas operation showed a rise of ~9% as the neutraliser gas flow rate changed from 20 mbar l/s to 30 mbar l/s. A calculation has been carried out for the total power loading and its distribution using particle tracking methods. The calculation of total

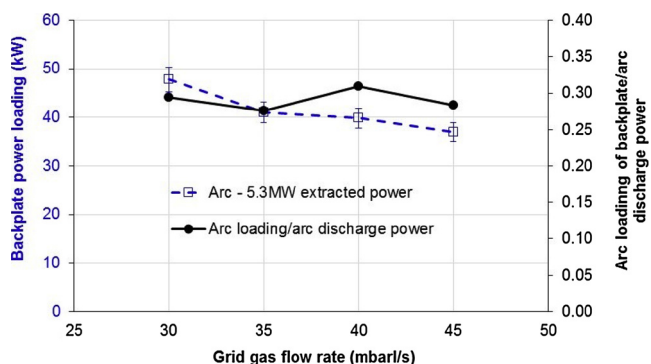


Fig. 17. Backplate loading due to the arc at 5.3 MW extracted power together with normalisation to the actual arc discharge power.

power striking the backplate is in reasonable agreement with the measured backplate loading. This may be somewhat fortuitous in this case. The empirical expression used to give the gas pressure in the accelerator, Eq. 4, for the case used in the calculation also estimates an increase in pressure at the earth grid and hence backplate loading of $\sim 28\%$ as the neutraliser gas flow is varied for 20 to 30 mbarl/s whereas the measurement shows only a $\sim 9\%$ increase. Eq. 4 has not been validated for the EP2 PINIs. The power distribution calculation is to be used in performing a thermo-mechanical analysis of the backplate to determine the cost in fatigue and lifetime of operating at higher neutraliser gas flow rates. Such an analysis may place operating limits on the PINI, however a complete redesign of the backplate cooling may have to be considered depending on available timescales.

In the case of grid gas operation, the variation in backplate loading from backstreaming electrons is much greater than for normal gas operation. Over the range of grid gas flow rates used the increase was $\sim 50\text{--}60\%$ compared to $\sim 9\%$ for normal gas operation. For the same total gas flow rate (ion source plus neutraliser and grid gas) the backplate load is less for grid gas operation at lower total gas flow rates and higher at higher total gas flow rates. In this case the increase in backplate loading over the range of grid gas flow rates is in good agreement with the prediction of Eq. 4. Operation at higher grid gas flow rates would then need to be carefully considered against potential benefits of improved neutralisation. The EP2 PINIs have not been operated in tritium gas as yet due to the fact that this cannot be done on the Test Bed. The operating regime and performance with tritium will have to be determined with initial experiments on JET prior to the experimental campaigns.

Declaration of Competing Interest

The authors declare that they have no known competing financial

interests or personal relationships that could have appeared to influence the work reported in this paper.

Acknowledgments

This work has been carried out within the framework of the Contract for the Operation of the JET Facilities and has received funding from the European Union's Horizon 2020 research and innovation programme. The views and opinions expressed herein do not necessarily reflect those of the European Commission.

References

- [1] D. Ćirić, et al., Performance of upgraded JET neutral beam injectors, *Fusion Eng. Des.* 86 (2011) 509–512, <https://doi.org/10.1016/j.fusengdes.2010.11.035>.
- [2] D.B. King, *Private Communication*, (2019).
- [3] T.T.C. Jones, et al., Tritium operation of the JET neutral beam systems, *Fusion Eng. Des.* 47 (1999) 205–231, [https://doi.org/10.1016/S0920-3796\(99\)00083-6](https://doi.org/10.1016/S0920-3796(99)00083-6).
- [4] R. McAdams, et al., Preparation for the next JET tritium campaign: performance of the EP2 PINIs with grid gas delivery, *Fusion Eng. Des.* 96–97 (2015) 527–531, <https://doi.org/10.1016/j.fusengdes.2015.01.043>.
- [5] P. Spädtke, AXCEL-INP, Junkernstr, Wiesbaden, Germany, 2019 99, 65205.
- [6] G. Fubiani, et al., Modelling of secondary emission processes in the negative ion based electrostatic accelerator of the International Thermonuclear Experimental Reactor, *Phys. Rev. ST Accel. Beams* 11 (2008) 014202, <https://doi.org/10.1103/PhysRevSTAB.11.014202>.
- [7] R.A. Baragiola, E.V. Alonso, A. Olivia Florio, Electron emission from clean surfaces induced by low energy light ions, *Phys. Rev. B* 19 (1979) 121–129, <https://doi.org/10.1103/PhysRevB.19.121>.
- [8] W. Arter, E. Surrey, D.B. King, The SMARDDA approach to ray-tracing and particle tracking, *IEEE Trans. Plasma Sci.* 43 (9) (2015) 3323–3331, <https://doi.org/10.1109/TPS.2015.2458897>.
- [9] W. Arter, Adaptive leapfrog scheme for charged particle sources, 25th International Conference on Numerical Simulation of Plasmas (2017).
- [10] D. Ćirić, PerMag Manual (Abingdon UKAEA Fusion/Euratom Association, Culham Science Centre) private communication, (2007).